EAI Endorsed Transactions
on Cognitive Communications
Research Article EAI.EU

Large-Signal Analysis and Characterization of a RF SOI-based Tunable Notch Antenna for LTE in TV White Space Frequency Spectrum

E. Ben Abdallah[1,*], S. Bories[1], D. Nicolas[1], A. Giry[1] and C. Delaveaud[1]

[1]CEA, LETI, MINATEC Campus, Univ. Grenoble-Alpes 38054 Grenoble, France

Abstract

The demand for spectrum resources has increased dramatically with the explosion of wireless mobile devices and services. The Cognitive Radio (CR) associated with TV white space frequencies defined between 470 MHz to 790 MHz is one solution to excel the spectrum resources shortage and address LTE low bands. The antenna design to cover such a wide band is a twofold challenge. First Electromagnetic fundamental limits impose a tradeoff between antenna efficiency, miniaturization and its frequency band wideness, secondly to be implemented in portable device (around 10 cm typical length) the antenna miniaturization needs is to be strong such as in λ/6 (where λ is the wavelength at 500 MHz). Thus, frequency reconfigurable antennas are suitable candidates and can be easy integrated. In this paper a compact frequency-agile notch antenna for LTE low-band using TV white space frequencies is designed and fabricated. The 18 x 3 mm notch size (area dedicated for the antenna) is only λ/33 at 500 MHz. The antenna aperture tuning is provided by a SOI CMOS tunable capacitor. The novelty of this paper is to present not only classical metrics (gain, return loss…) but also the experimental characterization of parameters that are usually used for active RF components. The non-standard tunable capacitor RF non linearity analysis is carried on and analyzed. The simulated and experimental performances are presented and demonstrate antenna tuning operation from 800 MHz down to 500 MHz. The slot electrical near field distribution is also investigated to confirm acceptable electrical field within the tunable component. High linearity is validated with measured ACLR levels lower than -30 dBc up to 22 dBm input power in the considered frequency range.

Keywords: Tunable notch antenna, TV white space, Tunable capacitor, LTE, linearity.

Received on 16 November 2016, accepted on 07 May 2017, published on 31 May 2017

doi: 10.4108/eai.31-5-2017.152558

1. Introduction

Due to the rapid demand for data over cellular networks, it has become difficult to cover all the traffic with current frequency bands. Thus, more frequency will be required to attend the increasing demand. However, it is becoming more and more challenging to allocate parts of spectrum for the data demand since most of the frequency bands which are suitable to mobile communications, are already assigned to the existing wireless systems.

The concept of Cognitive Radio (CR) proposed by [1] presents a solution to lower the usage of these widely used bands. The CR principles enable the unlicensed users to dynamically locate the unused spectrum segments and to communicate via these unused spectrum segments. CR used with TV White Space (TVWS) is one of solutions to excel spectrum resources shortage. TVWS are frequencies available for unlicensed use at locations where the spectrum is not being used by licensed services, such as television broadcasting. This spectrum is located from 470 MHz to 790 MHz in Europe [2].

*Corresponding author. Email: benabdallahassia@gmail.com

The antennas usually used for this band are geometrically large to cover the entire frequency band. Several wideband antennas have been proposed in these bands [3]. In [4], an asymmetric fork-like printed monopole antenna is presented for DVB-T application, which achieves a -10 dB bandwidth of 451-912 MHz but with a size of 247×35 mm^2. In [5], an UHF wideband printed monopole antenna has been introduced with dimension of 120×240 mm^2. Reconfigurable antennas, which are much more compact and have a low profile structures, are the most compelling for TVWS where instantaneous bandwidth is only a narrow part of the overall band.

In this paper a tunable miniaturized notch antenna [6] working in the TVWS bands is designed using a tunable capacitor. Since transmit RF circuits generally operate at high power level, linearity is a critical parameter to prevent distortions or inter-channel interferences. Therefore, a large signal analysis and characterization of the proposed tunable antenna has been performed by realizing adjacent channel leakage Ratio (ACLR) measurements on the antenna prototype using a LTE signal.

In the following sections, a frequency-agile notch antenna using a SOI CMOS tunable capacitor and addressing TVWS from 510 MHz to 900 MHz is studied, implemented and measured. First, TC tunable capacitor specifications are provided. Secondly, design, analysis and antenna measurements (impedance and efficiency) are presented. Then, near field of the notch antenna is studied in order to investigate antenna performances. Finally, a linearity analysis is performed.

2. Tunable Capacitor

2.1. Tunable Capacitor Design

The Tunable Capacitor (TC) used in this study is a Silicon-On-Insulator (SOI) CMOS integrated circuit based on a network of binary-weighted switched capacitors [7].

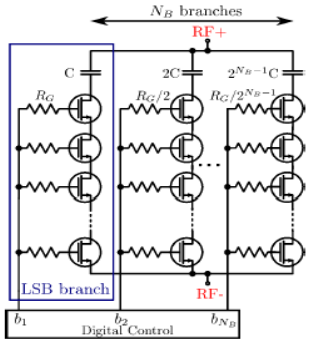

Figure. 1. Simplified schematic of the stacked-FET Tunable Capacitor

It is based on a network of N_B binary-weighted switched capacitors providing 2^{NB} capacitive states. Capacitors of the different branches follow a geometric progression with $C_{n+1} = 2C_n$, where n = 1 corresponds to the LSB branch. Figure. 1 shows the implementation of such tunable capacitor. Low-loss NFET-based switches select the appropriate capacitance value. As shown by Figure. 1, multiple FET transistors are stacked in series in order to evenly distribute the incoming high-power RF voltage across transistors and then prevent breakdown when operating in the OFF-state. Large gate resistors (R_G) are used to provide AC floating gates and avoid leakage of the RF signal into the digital control circuit.

2.1. Tunable Capacitor Characteristic

A 5-bit tunable capacitor has been designed under ADS simulation tool. The capacitance is digitally controlled through a SPI interface and it can be tuned from 1.3 pF to 7.1 pF at 1 GHz, Figure. 2.

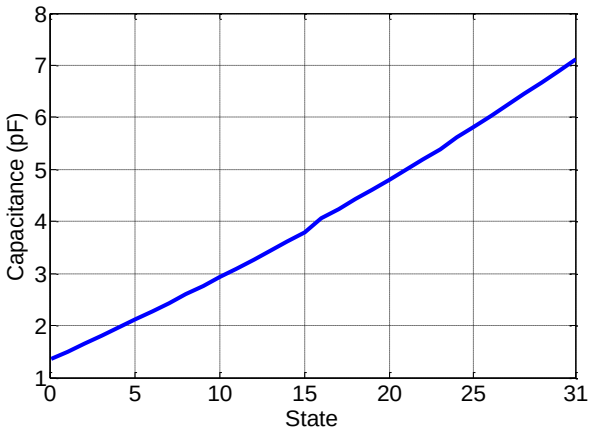

Figure. 2. Simulated Capacitance (@1 GHz) vs TC State in Shunt configuration

One of the most commonly emphasized electrical specifications for the tunable capacitor is the Quality Factor (Q), which is determined by the resistive (dissipative) losses of the component. Quality factor at 1 GHz versus tuning states is given in Figure. 3. It can be observed that a minimum quality factor of 40 is achieved for the highest TC state, whereas a maximum Q of 103 is obtained for the lowest state.

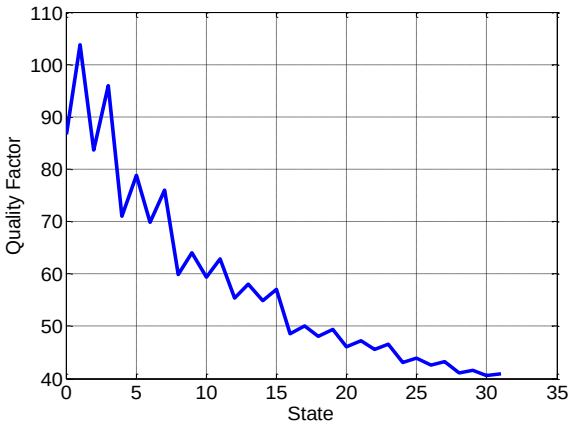

Figure. 3. Simulated quality factor (@1 GHz) vs TC State in Shunt configuration

3. Frequency-Reconfigurable Antenna

3.1. Antenna Design

The proposed antenna is a notch antenna designed on FR4 substrate (εr = 4.3, tg δ = 0.025) with a thickness of 0.8 mm. The slot size is 18 mm by 3 mm (which correspond to λ/32.6 by λ/196.7 at 510 MHz) etched on a ground plane size of 103 mm by 50 mm (λ/5.7 × λ/11.8 at 510 MHz), typical smartphone size [8]. The notch is closer to the PCB edge in order to free PCB central area and benefit from it to place battery and other components. Microstrip feeding line and control lines for the SOI tunable capacitor are located on the bottom layer. An open stub is set at the end of the microstrip line to match the antenna impedance (Figure. 4a). Orthogonal orientation and central positioning of the coaxial connector on the PCB helps to minimize interactions with measurement cable and disturbance of the radiated EM field as the surface currents are mainly located at the edges of the PCB, which contribute to the radiation. A small circuit powered by a miniature battery is used to maintain the tunable capacitor value during the anechoic chamber characterization (Figure. 4b). The tunable capacitor is positioned at the open end of the notch, where high electric fields are concentrated, to allow the antenna tuning at TVWS bands.

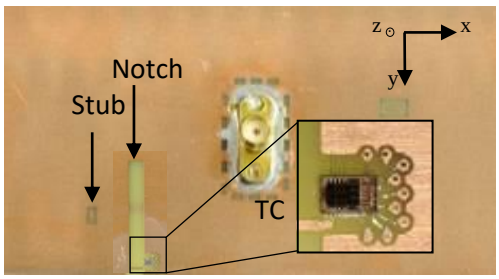

(a)

(b)

Figure. 4. Antenna structure (a) top view (b) bottom view

The simulated and measured input impedances are shown in Figure. 5. Below 2.2 GHz, simulation and measurement are similar. Above this frequency, a mean error of 15% is calculated and can be explained by losses introduced by manufactured materials. The unloaded antenna resonance frequency is 2.3 GHz which does not correspond to $\lambda_g/4$ due to the capacitive effect of the TC footprint at the open end of the slot. The antenna response is wideband.

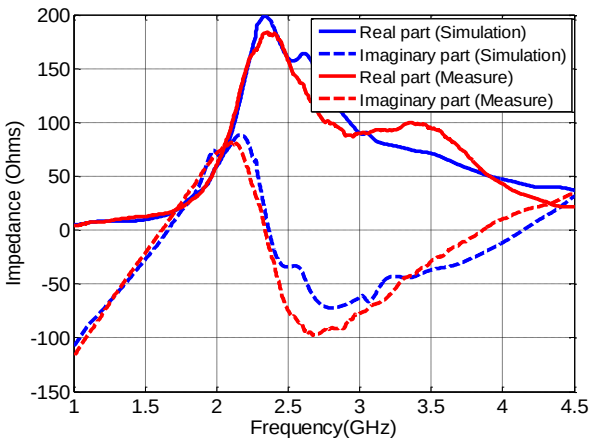

Figure. 5. Comparison of input impedance for the unloaded antenna

Figure. 6 presents the unloaded antenna radiation efficiency (η_r) simulated and measured. The measured efficiency is calculated from the integration of 2 cut-planes of the measured antenna total realized gain. It is important to note that radiation measurements are carried on without any metallic coaxial cable nor control interface not to perturb the antenna radiation and consequently the efficiency estimation. The measured efficiency is about 42% - 72%.

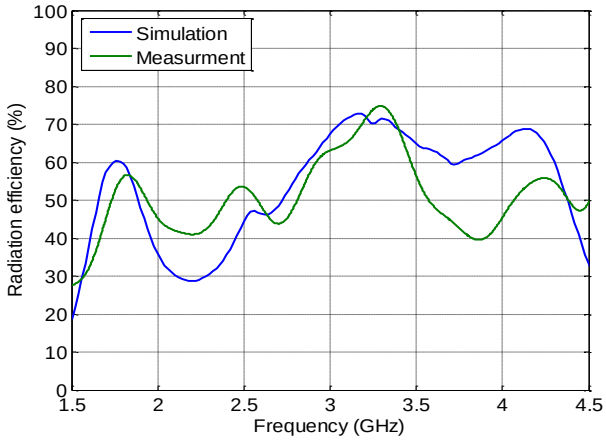

Figure. 6. Comparison of the antenna radiation efficiency

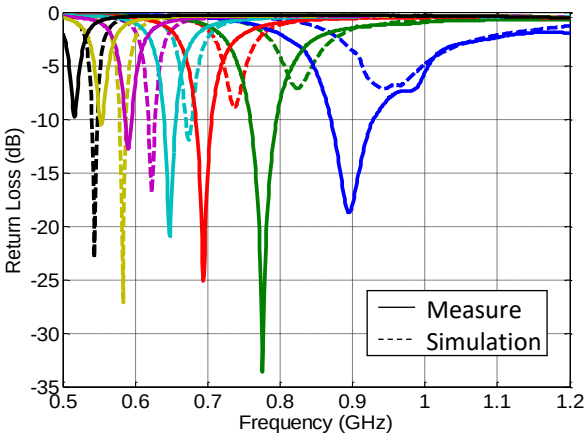

Figure. 8. Comparison of simulated and measured antenna response

3.2. Antenna Tuning

The tunable capacitor has been modeled under ADS and each state is imported into the EM simulator. Figure. 7 gives a comparison between simulation and measurement of the antenna response for a fixed capacitor connected at the end of the stub (Cstub = 1 pF) and different settings of the tunable capacitor. Simulated resonance frequency can be tuned from 550 MHz up to 960 MHz. The achievable bandwidth at -6 dB reflection coefficient ranges from 12 MHz to 70 MHz (Figure. 8) when operating frequency increases. The measured frequency response of the notch antenna for the different tunable capacitor settings ranges between 510 MHz and 900 MHz. A mean error of 8% is observed between the simulated and measured resonance frequency. This difference can be explained by some inaccuracies in the TC model.

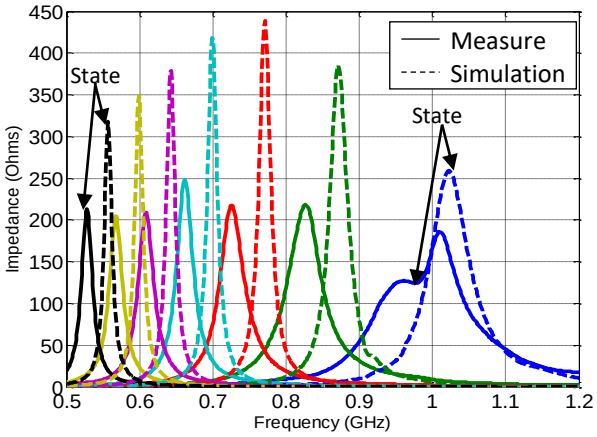

Figure. 7. Comparison of simulated and measured antenna input impedance (real part)

To address TVWS, a limited set of capacitor states (from 5 to 31) will be considered. Frequencies from 470 MHz to 510 MHz are not addressed with actual devise. It is so easily to cover them, just to use another tunable capacitor with a higher tuning ratio or to connect a fixed capacitor in parallel configuration.

The measured antenna radiation patterns including the co polarization and the cross polarization in both (xz) and (xy) plane at 510 MHz and 770 MHz are presented in Figure. 9. The gain is measured in the CEA-Leti anechoic chamber. The gain decreases, as expected, when the antenna is tuned to lower frequencies. At 770 MHz the notch length is λ/21 while at 510 MHz the notch is λ/32.6. In fact, as the antenna is tuned away from its natural resonance, higher currents run on the miniaturized surface and the series resistance of the tuning component causes higher insertion loss. Thus, it is a trade-off between antenna size, radiation performances and ESR. The radiation efficiency is affected by both the antenna size miniaturization and ESR value. In the following section the impact of both effects are analyzed.

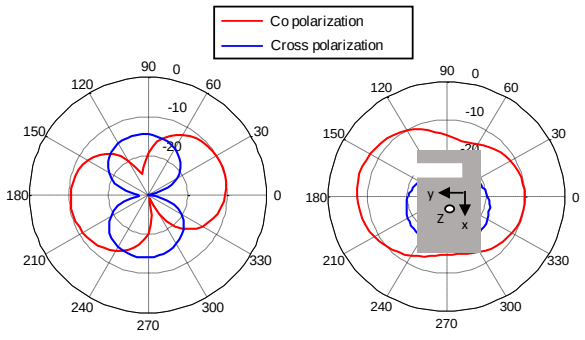

(a)

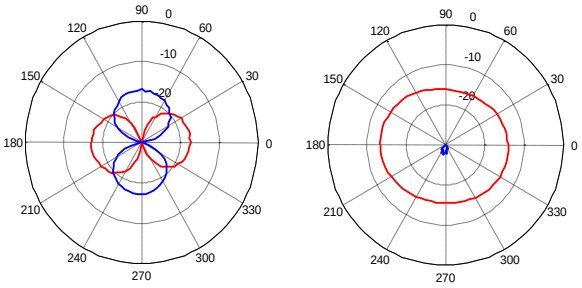

(b)

Figure. 9. Measured Radiation pattern (Realized Gain) of the antenna at (a) 790 MHz and (b) 510 MHz

As a result of the reduction in realized gain, a total efficiency (η_t) degradation is observed (-10 dB at 770 MHz). In order to demonstrate losses introduced by the ESR, an ideal TC (ESR=0 Ω) was simulated and results indicate that for state 5 (capacitance is equal to 2.1 pF) the antenna resonance frequency is 770 MHz and corresponding total efficiency is -2.5 dB and for state 31 (C= 5.5 pF), total efficiency is -5.8 dB. Equally at low frequency, the antenna is miniaturized and consequently, bandwidth and efficiency decrease as predicted by the fundamental limits of electrically small antennas [8], these are the losses of the finite conductivity. Introducing ESR values, the efficiencies decrease significantly. For ESR= 3 Ω, at 770 MHz η_t is reduced by 3 dB and at 510 MHz, the efficiency is reduced by 7.5 dB. The ESR effect is more intense for low frequencies. In fact, more the antenna is miniature, high currents run on it and the ohmic losses which are proportional to the square of this high currents increase and cause higher efficiency degradation. Considering the real TC ESR, the efficiency decreases about 7.5 dB for state 5. Thus, until new generation of TC that exhibit lower ESR one solution could be the use of a fixed capacitor in parallel with the TC. Using this method, the ESR value can be reduced and currents will be split between the two capacitors.

3.3. Near field Measurement

To visualize the electrical field around the notch, it was measured at several frequencies at a distance of 2 mm above the PCB with an optical probe [9] and with a 1 mm spatial sampling in the x and y directions around the slot area. The Vector Network Analyzer (VNA) is used to measure the received power of the probe's output. Figure. 10 shows the measurement setup. The polarized probe is oriented to measure a given E field component. The input power is fixed for -10 dBm.

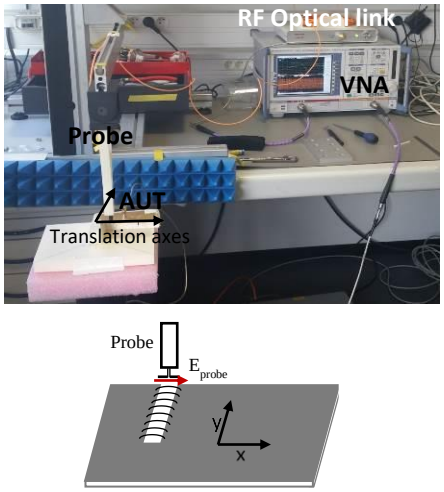

Figure. 10. Demonstrator setup

According to Babinet's principle [10] which relates the radiated fields and impedance of a slot antenna to that of its dual antenna. The dual of a slot is a dipole antenna, the conductive material and the air were interchanged. Thus, E-field and H-field are interchanged. Since the dipole-fields are well known, the slot fields are also and its E-field is mainly within X. Figure. 11 shows the total E-field measurements and simulations at 560 MHz.

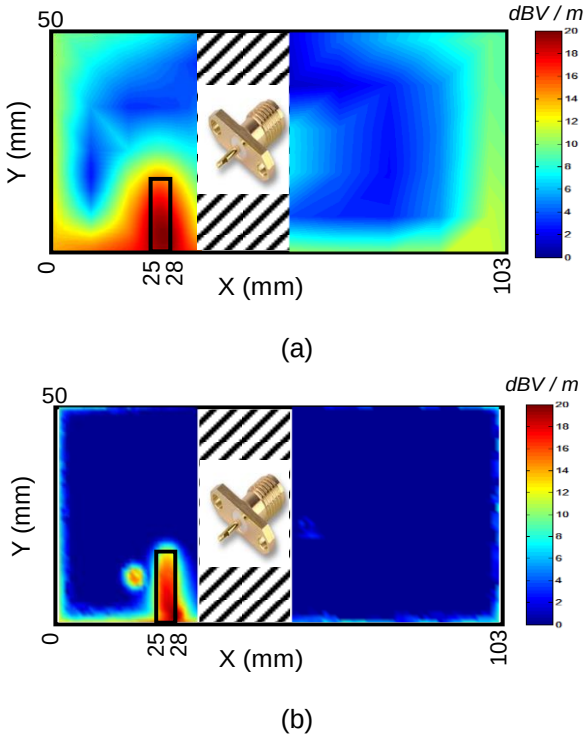

(a)

(b)

Figure. 11. Total E-field (dBV/m) of the notch antenna at 560 MHz (a) Measurement (b) Simulation

The field is maximum at the slot edge and especially at the slot open end. In measurement, high field is clearly located on the PCB edges which presents a difference from simulation. This difference is explained by the lower spatial resolution of the measuring probe and also the spatial sampling which is not accurate especially away from the slot area (10 mm spatial sampling) than in the simulation mesh. To visualize clearly the electrical field level in the slot, Figure. 12 presents the total E level along the slot (Y slot range is between 0 to 50 mm) at 560 MHz for two positions in the notch x_1 and x_2, x_1 corresponds to 26 mm and x_2 is 27 mm. In this section, the focus will not be on differences between simulation and measurement but on the field distribution on the antenna. y=0 mm corresponds to the slot open end. A 2 mm from the open end, where the TC is implemented, an electrical field peak is observed in both measurements and simulations. The field decreases significantly from the open end to the slot short end of about 95%. At the PCB edge (y around 50 mm) the field re-increases (lesser than level in the notch) which demonstrates that PCB edges contribute to the antenna radiation. The same E-field distribution profile is observed in simulation and measurement.

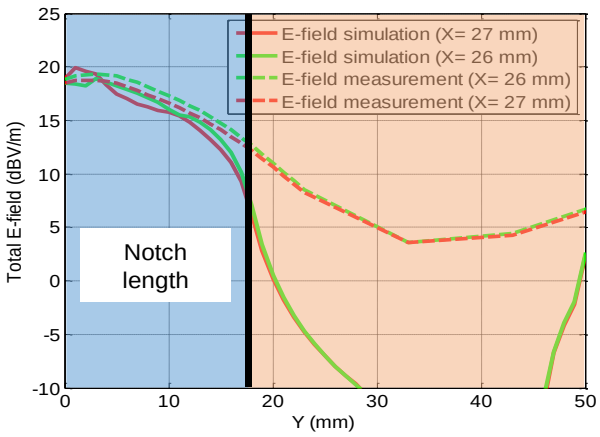

Figure. 12. E-field (dBV/m) along the notch at 560 MHz

To demonstrate that the field is higher at the resonance frequency and much lower away, E-field is measured at 500 MHz, 560 MHz (the resonance frequency), and 600 MHz. At 500 MHz, E-Field is 6 dBV/m lesser than the level at the resonance frequency and 4 dBV/m at 600 MHz.

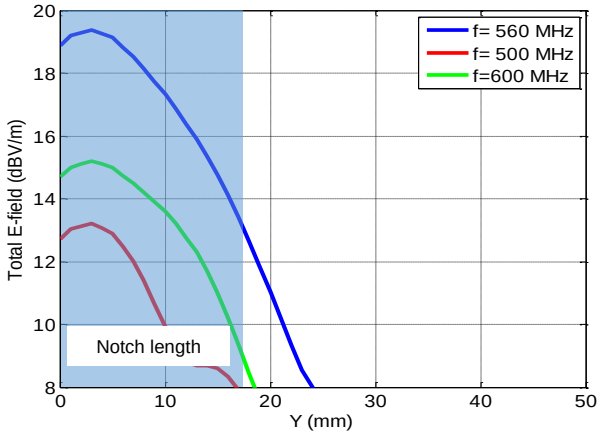

Figure. 13. Measured E-field (dB) along the notch at 500 MHz, 560 MHz and 600 MHz

4. Analysis and characterization of tunable antenna linearity

One critical specification for digital communication systems is the Adjacent Channel Leakage Ratio (ACLR) corresponding to signal distortion leaking in neighboring channels. Leakage power influences the system capacity as it interferes with the reception in adjacent channels. Therefore it must be rigorously controlled to guarantee correct communication for all subscribers in a network. ACLR is the ratio of the power in the adjacent channels to the power in the transmit channel. ACLR limits are imposed by the 3GPP standard for the whole system, however up to now there are no specific constraints for the antenna. Compared to the typical two ports antenna characterization, antenna linearity characterization has to be carried over the air (OTA).

4.1. ACLR Measurement Setup

ACLR measurements are made using a spectrum analyzer and the required test signals are built using a signal generator. In the following setup, a Vector Signal Generator with an internal baseband generator is connected to the antenna in transmission to allow generation of a LTE signal and the received signal from the measurement (Horn) antenna is connected to a Spectrum Analyzer (Figure. 14). For LTE, depending on the considered signal bandwidth, the adjacent channels are located at ±1.4 MHz, ±3 MHz, ±5 MHz, ±10 MHz, ±15 MHz and ±20 MHz offsets [11].

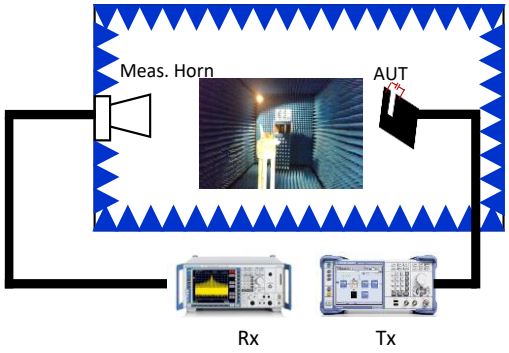

Figure. 14. Measurement setup around the anechoic chamber

4.2. ACLR Measurement Results

Figure. 15 shows the measured ACLR characteristic of the tunable antenna for state 5 and a 16 QAM LTE 10 MHz uplink signal at 770 MHz for different antenna input power (Pin) ranging from 5 dBm to 23 dBm. Dotted line corresponds to the noise floor. As can be seen, ACLR level increases linearly with the input power and can be approximated by the following equation: [3.5 Pin -106] (dBc). The tunable antenna respects the standard ACLR specification of -30dBc up to 22 dBm input power at 770 MHz.

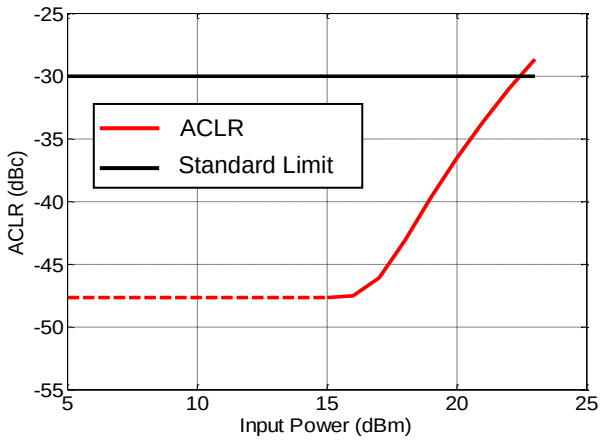

Figure. 15. Measured ACLR versus input power with a LTE 16 QAM 10 MHz signal at 770 MHz

ACLR is measured for different TC states and frequencies using an LTE 16 QAM 10 MHz uplink signal. Table I summarizes the linearity performance of the tunable antenna.

Table 1. Measured power at the input of the tunable antenna for ACLR=-30dBc

State Frequency	State 5 770 MHz	State 10 685 MHz	State 15 630 MHz	State 31 510 MHz
Pin (ACLR= -30 dBc)	22 dBm	22 dBm	23 dBmt	22 dBm

The tunable antenna respect the standard specification up to 22 dBm input power which corresponds to the LTE UE transmit power as specified in 3GPP TS36.101 (UE core specification) [11].

5. Conclusion

In this paper, a miniature tunable notch antenna is proposed to address LTE low bands in TVWS spectrum. The notch antenna incorporates a SOI CMOS tunable capacitor at its open-end to operate in the different communication bands ranging from 510 MHz to 900 MHz. Measured results demonstrate trade-off between compact size, limited instantaneous operating bandwidth and radiation efficiency. The notch near field distribution has been investigated in order to predict the E-field level for a given input power which is a major limitation in the TC design. The RF linearity characterization of the tunable antenna has been performed through ACLR measurements on the antenna prototype and obtained results demonstrate that the proposed tunable antenna respects the standard specifications. Due to the dynamic frequency allocation within TVWS, fast transition times between frequency bands are expected to satisfy high quality communications, around 5.5 µs. At last, notice the proposed antenna solution is not restricted to LTE but is also compatible with other waveforms.

References

[1] J. Mitola III, “Cognitive Radio”, Ph.D. thesis, KTH, Stockholm, Sweden, 2000.

[2] Mueck, M.; Noguet, D., "TV White Space standardization and regulation in Europe," in Wireless Communication, Vehicular Technology, Information Theory and Aerospace & Electronic Systems Technology (Wireless VITAE), 2011 2nd International Conference on , vol., no., pp.1-5, Feb. 28 2011-March 3 2011.

[3] John, M.; Ammann, M.J., "A compact shorted printed monopole antenna for TV white space trials," in Antennas and Propagation (EuCAP), 2013 7th European Conference on , vol., no., pp.3713-3715, 8-12 April 2013.

[4] C. Huang, B. Jeng, and C. Yang, “Wideband monopole antenna for DVB-T applications,” Electronics Letters, vol. 44, 2008, pp. 1448-1450.

[5] Xianling Liang; Ronghong Jin; Yue Zhao; Junping Geng, "Compact DVB-T printed monopole antenna," in Antenna Technology (iWAT), 2010 International Workshop on , vol., no., pp.1-4, 1-3 March 2010.

[6] Le Fur, G.; Lach, C.; Rudant, L.; Delaveaud, C., "Miniature reconfigurable multi-antenna system for IMT-Advanced band," in IEEE International Symposium on Antennas and Propagation (APSURSI), vol., no., pp.1207-1210, 3-8 July 2011.

[7] Nicolas, D.; Giry, A.; Ben Abdallah, E.; Bories, S.; Tant, G.; Parra, T.; Delaveaud, C.; Vincent, P.; Po, F.C.W., "SOI CMOS tunable capacitors for RF antenna aperture tuning," in Electronics, Circuits and Systems (ICECS), 2014 21st IEEE International Conference on , vol., no., pp.383-386, 7-10 Dec. 2014.

[8] L. J.Chu, "Physical limitations on omni-directional antennas", J. Appl. Phys., vol. 19, pp. 1163-1175, Dec. 1948.

[9] http://www.enprobe.de/datasheets/EFS-105.pdf

[10] H.G Booker, “Slot Aerials and Their Relation to Complementary Wire Aerials, “ JIEE (Lond.), 93, pt. IIIA, no. 4, 1946.

[11] http://www.etsi.org/deliver/etsi_ts/136199/136/101/10.03.00/ts_136101v100300.pdf.